GDI-1 Phosphorylation Switch at Serine 96 Induces RhoA Activation and Increased Endothelial Permeability[▽]

Nebojsa Knezevic, Arun Roy, Barbara Timblin, Maria Konstantoulaki, Tiffany Sharma, Asrar B. Malik, and Dolly Mehta*

Department of Pharmacology and Center for Lung and Vascular Biology, College of Medicine, University of Illinois, Chicago, Illinois

We identified the GDI-1-regulated mechanism of RhoA activation from the Rho–GDI-1 complex and its role in mediating increased endothelial permeability. Thrombin stimulation failed to induce RhoA activation and actin stress fiber formation in human pulmonary arterial endothelial cells transduced with full-length GDI-1. Expression of a GDI-1 mutant form (C-GDI) containing the C terminus (aa 69 to 204) also prevented RhoA activation, whereas further deletions failed to alter RhoA activation. We observed that protein kinase Cα-mediated phosphorylation of the C terminus of GDI-1 at Ser96 reduced the affinity of GDI-1 for RhoA and thereby enabled RhoA activation. Rendering GDI-1 phosphodefective with a Ser96 → Ala substitution rescued the inhibitory activity of GDI-1 toward RhoA but did not alter the thrombin-induced activation of other Rho GTPases, i.e., Rac1 and Cdc42. Phosphodefective mutant GDI-1 also suppressed myosin light chain phosphorylation, actin stress fiber formation, and the increased endothelial permeability induced by thrombin. In contrast, expressing the phospho-mimicking mutant S96D-GDI-1 protein induced RhoA activity and increased endothelial permeability independently of thrombin stimulation. These results demonstrate the crucial role of the phosphorylation of the C terminus of GDI-1 at S96 in selectively activating RhoA. Inhibiting GDI-1 phosphorylation at S96 is a potential therapeutic target for modulating RhoA activity and thus preventing the increase in endothelial permeability associated with vascular inflammation.

The monomeric Rho GTPase RhoA plays a critical role in regulating cell migration, contraction, growth, and apoptosis (28, 36). Guanine nucleotide dissociation inhibitors (GDIs) bind with the GDP form of Rho GTPases and prevent their dissociation from the complex. Thus, Rho-GDI interaction serves as a primary means for limiting Rho GTPase activation (3, 5, 6, 23). GDIs also stimulate the release of Rho GTPases from cell membranes, thereby contributing to inactivation of the Rho GTPase cycle (3, 5, 6, 23). Rho–GDI-1 is a ubiquitously expressed member of the Rho-GDI family (3, 5, 6, 23). Deletion of GDI-1 in mice resulted in death within 6 months because of renal failure resulting in proteinuria (33). Studies of mesangial cells from Rho–GDI-1$^{-/-}$ mice showed increased actin stress fiber formation (17), suggesting that endogenous GDI-1 serves an important function in modulating RhoA activity.

RhoGDI-1 is composed of a flexible 69-amino-acid (aa) N terminus and an immunoglobulin-like, folded, 135-aa C terminus (8, 11, 18). The N terminus contains the nucleotide binding site, and the C terminus contains a hydrophobic pocket that binds the isoprenyl group of Rho GTPases (9, 11, 18). In vitro studies showed that GDI-1 mutant protein containing the C-terminal domain binds Cdc42 but has little effect on the rate of GDP dissociation from Cdc42 (9). Thus, GDI-1 C terminus binding to Rho GTPases may be an

important factor limiting their activation. However, mechanisms of GDI-1 C terminus regulation of Rho GTPase activity (e.g., the role of phosphorylation of GDI-1 and protein interactions) are incompletely understood. The N-terminal domain of radixin, a member of the ezrin-radixin-moesin (ERM) family of proteins, binds the C terminus of Rho GDI-1 (10). Transduction of radixin's N terminus in fibroblasts resulted in RhoA-dependent actin stress fiber formation (27), suggesting a role for radixin interaction in the modulating GDI-1 inhibition of Rho GTPases. Phosphorylation of GDI-1 by p21-activated kinase (PAK) at the C terminus induced the dissociation of Rac1 from the Rac1–GDI-1 complex (4), suggesting that PAK-mediated phosphorylation of GDI-1 at the C terminus may be an another important mechanism of Rho GTPase activation.

Thrombin, by binding to endothelial cell surface *p*rotease-*a*ctivated *r*eceptor 1 (PAR-1), induces the development of minute interendothelial junctional gaps that lead to increased endothelial permeability, the hallmark of vascular inflammation (19). RhoA activation is required in signaling the increase in endothelial permeability (19). We have shown that PAR-1 stimulation induced RhoA activation within minutes secondary to protein kinase Cα (PKCα)-mediated GDI-1 phosphorylation (20). To identify the switch mechanism responsible for GDI-1-mediated RhoA activation, in the present study we expressed full-length (FL; aa 1 to 204) GDI-1 or the C terminus (aa 69 to 204) of GDI-1 in endothelial cells. We demonstrated by mutational analysis the essential requirement for GDI-1 C-terminal Ser96 phosphorylation in regulating RhoA activation. PKCα-mediated phosphorylation at GDI-1 Ser96

induced RhoA activation and thereby signaled an increase in endothelial permeability.

MATERIALS AND METHODS

Materials. Human pulmonary arterial endothelial (HPAE) cells and endothelial growth medium (EBM-2) were obtained from Clonetics (San Diego, CA). Human α-thrombin was obtained from Enzyme Research Laboratories (South Bend, IN). Superfect and DEAE-dextran transfection reagents were purchased from QIAGEN (Valencia, CA), whereas Lipofectamine 2000 transfection reagent was obtained from Invitrogen (Carlsbad, CA). The Nucleofector HCAEC kit and electroporation system were from Amaxa (Gaithersburg, MD). Alexa-labeled phalloidin, 4′,6′-diamidino-2-phenylindole (DAPI), and ProLong Gold antifade were from Molecular Probes (Eugene, OR). Glutathione-Sepharose 4B and [γ-^{32}P]ATP were purchased from Amersham Biosciences (Piscataway, NJ). Electrodes for transendothelial electrical resistance (TER) measurements were obtained from Applied Biosciences (Troy, NY). Anti-green fluorescent protein (anti-GFP) and horseradish peroxidase-conjugated anti-mouse immunoglobulin G (IgG) antibodies (Abs) and protein A/G beads were purchased from Santa Cruz Biotechnology (San Diego, CA). Anti-RhoA, -Cdc42, and -Rac1 Abs were purchased from BD Biosciences (San Jose, CA). Antihemagglutinin (anti-HA) Ab was from Roche Chemicals (Indianapolis, IN). Fc fragment-specific, horseradish peroxidase-conjugated anti-mouse IgG Ab was purchased from Jackson ImmunoResearch Laboratories (West Grove, PA). Recombinant PKCα, glutathione S-transferase (GST)-rhotekin-Rho binding domain beads, and PAK-binding domain–GST beads were purchased from Cytoskeleton (Denver, CO).

Endothelial cell culture. HPAE cells were cultured in a T-75 flask coated with 0.1% gelatin in EBM-2 medium with 10% fetal bovine serum and maintained at 37°C in a humidified atmosphere of 5% CO_2 and 95% air until they formed a confluent monolayer. Cells from each of the primary flasks were detached with 0.05% trypsin containing 0.02% EDTA for the indicated experiments. In all of the experiments, unless otherwise indicated, a confluent monolayer of HPAE cells was washed twice with serum-free MCDB-131 medium and incubated in the same serum-free medium for 1 h before treatment with thrombin. In all of the experiments, HPAE cells between passages 5 and 8 were used.

Construction of GFP-tagged mutant GDI-1 proteins. Rho GDI-1 fragments were generated by PCR amplification (*Pfu*; Stratagene) with the cDNA clone pOTB7-GDI-1 as the template. Agarose gel-purified PCR fragments were digested with restriction enzymes EcoRI/BamHI or EcoRI/XhoI and cloned into vector pEGFP-C3. All subsequent clones were sequenced to ensure sequence integrity. The clone-specific primer pairs used were the pEGFP-FL GDI-1 mutant (aa 1 to 204) forward primer 5′-AGGAATTCGAATGGCTGAGCAGGA GCCCAC-3′ and reverse primer 5′-CGGGATCCTCATCAGTCCTTCCAGTC CTTC-3′, the pEGFP-C-GDI-1 mutant (aa 69 to 204) forward primer 5′ AGG AATTCGAAACGTCGTGGTGACTGG 3′ and reverse primer 5′ CGGGATC CTCATCAGTCCTTCCAGTCCTTC 3′, the pEGFP-C1-GDI-1 mutant (aa 69 to 140) forward primer 5′-AGGAATTCGAAACGTCGTGGTGACTGG-3′ and reverse primer 5′-CGGGATCCTCATCAGTCAATCTTGACGCCTTTCC-3′, and the pEGFP-C2-GDI-1 (aa 141 to 204) forward primer 5′-AGGAATTCGA AAGACTGACTACATGGTAGGC-3′ and reverse primer 5′-CGGGATCCTC ATCAGTCCTTCCAGTCCTTC-3′. Phosphorylation-defective mutant proteins were generated through a two-step PCR process. In short, overlapping DNA fragments containing base pair changes were generated in separate PCRs during the first round of PCR with the cDNA clone pOTB7-GDI as the template. These fragments were combined and used as the second-round PCR template to amplify the entire GDI-1 cDNA containing the specific amino acid changes. Agarose gel-purified PCR fragments were digested with the EcoRI/BamHI restriction enzymes and cloned into pEGFP-C3. Subsequent clones were sequenced to ensure sequence integrity. The clone-specific primer pairs used, with amino acid changes in bold and underlined, were pEGFP-S96A C1-GDI-1 (first-round PCR primer pairs) forward primer 1 (5′-AGGAATTCGAATGGCTGAGCAGGAG CCCAC-3′), reverse primer 1 (5′-TTCTTGAAG**GC**CTCCAGGTCGC-3′), forward primer 2 (5′-ACCTGGAGG**GC**CTTCAAGAAGC-3′), and reverse primer 2 (5′-CGGGATCCTCATCAGTCCTTCCAGTCCTTC-3′) (the second-round PCR used forward primer 1 and reverse primer 2); pEGFP-S176A-C2-GDI-1 (first-round primer pairs) forward primer 1 (5′-AGGAATTCGAATG**G**CTGA GCAGGAGCCCAC-3′), reverse primer 1 (5′-GCGGGACTTGATGGCGTAG C-3′), forward primer 2 (5′-AGCTAC**GC**CATCAAGTCCCGC-3′), and reverse primer 2 (5′-CGGGATCCTCATCAGTCCTTCCAGTCCTTC-3′) (the second-round PCR used forward primer 1 and reverse primer 2); pEGFP-T197A-C2-GDI-1 (first-round primer pairs) forward primer 1 (5′-AGGAATTCGAATGG CTGAGCAGGAGCCCAC-3′), reverse primer 1 (5′-TCCTTCTTGATGG**C**G AGATTCC-3′), forward primer 2 (5′-AATCTC**G**CCATCAAGAAGGAC-3′),

and reverse primer 2 (5′-CGGGATCCTCATCAGTCCTTCCAGTCCTTC-3′) (the second-round PCR used forward primer 1 and reverse primer 2); pEGFP-S96A-FL GDI-1 (first-round primer pairs) forward primer 1 (5′-AGGAATTC GAATGGCTGAGCAGGAGCCCAC-3′), reverse primer 1 (5′-TTCTTGAAG **GC**CTCCAGGTCGC-3′), forward primer 2 (5′-ACCTGGAGG**GC**CTTCAAGA AGC-3′), and reverse primer 2 (5′-CGGGATCCTCATCAGTCCTTCCAGTC CTTC-3′) (the second-round PCR used forward primer 1 and reverse primer 2); pEGFP-S96D-FL GDI-1 (first-round primer pairs) forward primer 1 (5′-AGG AATTCGAATGGCTGAGCAGGAGCCCAC-3′), reverse primer 1 (5′ GACT GCTTCTTGAAG**GT**CTCCAGGTCGCC-3′), forward primer 2 (5′-GGCGAC CTGGAGG**GA**CTTCAAGAAGCAGTC-3′), and reverse primer 2 (5′-CGGGA TCCTCATCAGTCCTTCCAGTCCTTC-3′) (the second-round PCR used forward primer 1 and reverse primer 2); pEGFP-S176A-FL GDI-1 (first-round primer pairs) forward primer 1 (5′-AGGAATTCGAATGGCTGAGCAGGAG CCCAC-3′), reverse primer 1 (5′-GCGGGACTTGATG**G**GCGTAGC-3′), forward primer 2 (5′-AGCTAC**GC**CATCAAGTCCCGC-3′), and reverse primer 2 (5′-CGGGATCCTCATCAGTCCTTCCAGTCCTTC-3′) (the second-round PCR used forward primer 1 and reverse primer 2); and pEGFP-T197A-FL GDI-1 (first-round primer pairs) forward primer 1 (5′-AGGAATTCGAATGG CTGAGCAGGAGCCCAC-3′), reverse primer 1 (5′-TCCTTCTTGATGGC**G** AGATTCC-3′), forward primer 2 (5′-AATCTC**G**CCATCAAGAAGGAC-3′), and reverse primer 2 (5′-CGGGATCCTCATCAGTCCTTCCAGTCCTTC-3′) (the second-round PCR used forward primer 1 and reverse primer 2).

Cell transfection. cDNA was purified with the Endo-free QIAGEN kit and transduced into cells by electroporation or with Superfect transfection reagent. HPAE cells grown to 70% confluence were trypsinized and mixed with 4 μg of cDNA along with 100 μl of HCAEC nucleofector solution. Cells were rapidly electroporated with an Amaxa nucleofector device in accordance with the manufacturer's recommended program (S-05). Electroporated cells were mixed in EBM-2 and plated on 60-mm dishes. HPAE cells plated onto gold electrodes or 12-mm coverslips were transfected with the indicated cDNA with Superfect transfection reagent in accordance with the manufacturer's protocol. The cells were used after 24 h of transfection, when there was clear evidence of the expression of protein. COS-7 cells were cultured in Dulbecco's modified Eagle's medium supplemented with 10% fetal bovine serum. COS-7 cells were transfected with appropriate cDNA with Lipofectamine 2000 by following the manufacturer's protocol.

Serum response element (SRE) reporter gene activity. Transfections were made by the DEAE-dextran method as previously described (20). Following serum deprivation, cells were stimulated with 50 nM α-thrombin for 5 h. Cell extracts were prepared and assayed for luciferase activity with the Dual Luciferase Reporter Assay System (Promega). SRE-luciferase activity was expressed as the ratio of firefly to *Renilla* luciferase activities.

Actin stress fiber staining. Following stimulation with thrombin, cells were fixed and incubated with Alexa-labeled phalloidin to stain actin stress fibers. Cells were viewed with a 63× 1.2 NA objective and a Zeiss LSM 510 confocal microscope (13).

Measurements of Rho GTPase activity. HPAE cells transducing the indicated cDNA were stimulated with 50 nM thrombin. RhoA activity was measured with GST-rhotekin-Rho binding domain, whereas GST-PAK binding domain was used to quantify Rac and Cdc42 activities as previously described (13, 20).

TER measurement. The time course of endothelial cell retraction in real time, a measurement of increased endothelial permeability via the paracellular pathway, was measured as previously described (13, 20).

Immunoprecipitation. HPAE cells or COS-7 cells were washed with phosphate-buffered saline and lysed with radioimmunoprecipitation assay buffer (1% Triton X-100, 150 mM NaCl, 10 mM Tris, 1 mM EDTA, 1 mM EGTA, 1 mM Na_3VO_4, 1 mM phenylmethylsulfonyl fluoride, 0.5% Nonidet P-40, and 2 μg/ml each pepstatin A, leupeptin, and aprotinin) (13, 20). The lysate was cleared by centrifugation at 4°C at 14,000 × g for 10 min. Cell lysate was then precleared with protein A/G-agarose beads for 30 min, and the proteins were immunoprecipitated with the appropriate Ab overnight at 4°C, followed by incubation with protein A/G-agarose for 6 h at 4°C. The beads were then collected by centrifugation and washed three times with detergent-free radioimmunoprecipitation assay buffer.

In vitro kinase assay. COS 7 cells transducing various mutant GDI-1 proteins were lysed and immunoprecipitated with anti-GFP Ab. The beads were incubated with purified PKCα to determine phosphorylation as previously described (20).

Statistical analysis. Comparisons between experimental groups were made by analysis of variance and t test with SigmaStat software. Differences in mean values were considered significant at $P < 0.05$.
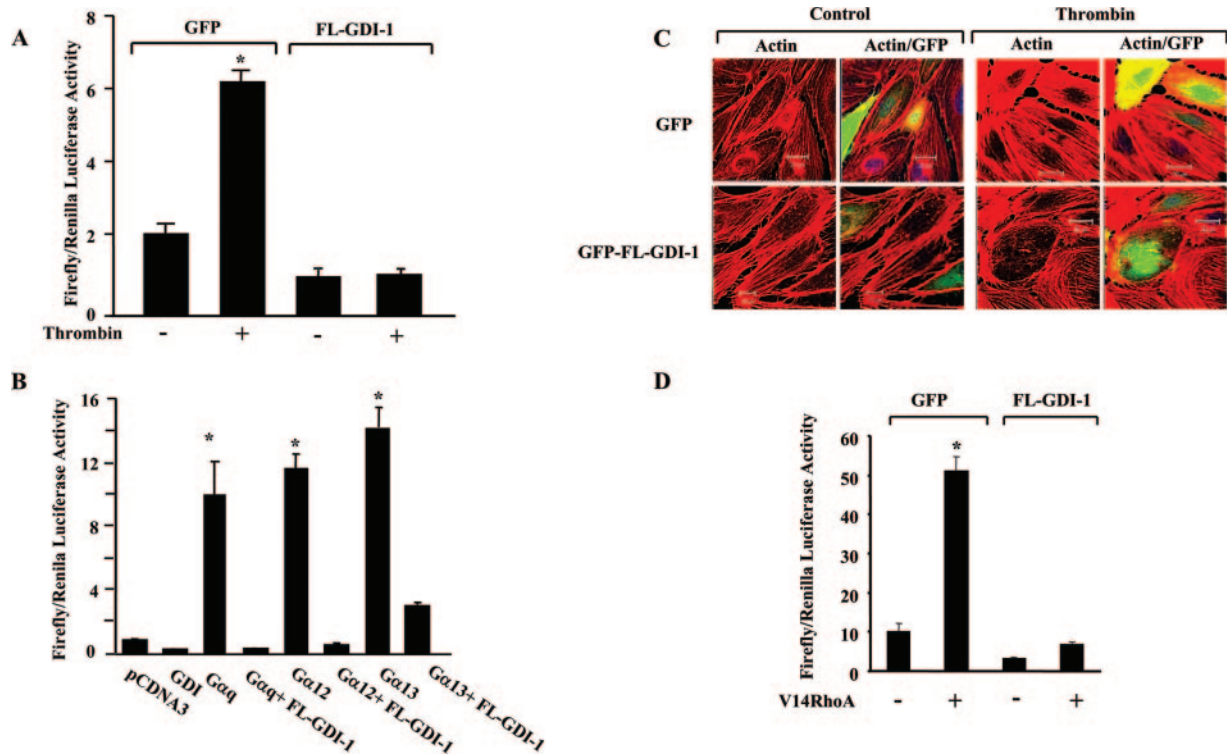
FIG. 1. GDI-1 expression prevents SRE activation and actin stress fiber formation. (A) Effect of GDI-1 on SRE activity induced by thrombin. HPAE cells were cotransfected with an SRE-luciferase plasmid and GFP or GFP-tagged FL GDI-1. Cells were then stimulated with thrombin for 5 h prior to SRE activity measurement with a dual-reporter assay kit. SRE-luciferase activity is expressed as the ratio of firefly to *Renilla* luciferase activities. Data represent the mean ± the standard deviation from four experiments performed in triplicate. Asterisks indicate values different from those obtained with unstimulated vector-expressing cells or cells expressing FL GDI-1 with or without thrombin stimulation ($P < 0.05$); +, presence; −, absence. (B) Effect of GDI-1 on SRE activity induced by constitutively active heterotrimeric G proteins. HPAE cells were cotransfected with constitutively active $G\alpha_q$, $G\alpha_{12}$, or $G\alpha_{13}$ mutant with or without FL GDI-1, and SRE reporter activity was determined. SRE-Luc activity is expressed as the ratio of firefly to *Renilla* luciferase activities. Data represent the mean ± the standard deviation from three experiments performed in triplicate. Asterisks indicate values different from those obtained with vector-expressing cells or cells coexpressing FL GDI-1 and constitutively active $G\alpha$ subunits ($P < 0.05$). (C) Effect of GDI-1 on thrombin-induced actin stress fiber formation. HPAE cells transfected with GFP or GFP–GDI-1 were stimulated with 50 nM thrombin for 5 min, after which cells were fixed and stained with phalloidin to determine actin stress fiber formation. Results are representative of at least three experiments. (D) Effect of GDI-1 on SRE activation induced by constitutively active RhoA. HPAE cells were cotransfected with constitutively active RhoA (V14RhoA) with or without FL GDI-1, and SRE reporter activity was determined. SRE-Luc activity is expressed as the ratio of firefly to *Renilla* luciferase activities. Data represent the mean ± the standard deviation from three experiments performed in triplicate. Asterisks indicate values significantly higher in cells expressing constitutively active RhoA (V14 RhoA) than in cells expressing the vector alone or coexpressing V14RhoA and FL GDI-1 ($P < 0.05$); +, presence; −, absence.

RESULTS

GDI-1 expression prevents SRE activation and actin stress fiber formation induced by thrombin. We measured SRE activation to determine the role of FL GDI-1 in regulating RhoA-induced SRE activity. Thrombin stimulation induced marked SRE activation in GFP-transducing HPAE cells but not in cells transduced with FL GDI-1 (Fig. 1A).

Because the $G\alpha_{12}$, $G\alpha_{13}$, and $G\alpha_q$ heterotrimeric GTP binding proteins can mediate RhoA activation downstream of G-protein-coupled receptors (1, 13, 16, 21, 34), we addressed the role of FL GDI-1 in signaling $G\alpha_q$-, $G\alpha_{12}$-, or $G\alpha_{13}$-mediated SRE activation. Transducing constitutively active mutant forms of $G\alpha_q$, $G\alpha_{12}$, or $G\alpha_{13}$ into HPAE cells increased SRE activity; however, coexpression of either $G\alpha_q$, $G\alpha_{12}$, or $G\alpha_{13}$ with GDI-1 prevented SRE activation (Fig. 1B). Thus, GDI-1 plays a central role in inducing SRE activation downstream of $G\alpha_q$, $G\alpha_{12}$, and $G\alpha_{13}$.

As RhoA activation regulates actin stress fiber formation, we

determined alterations in actin stress fibers in response to thrombin challenge of GFP- or GFP–GDI-1-transducing HPAE cells. Confocal microscopy showed that thrombin induced actin stress fiber formation in cells transduced with the control vector but not in cells transduced with FL GDI-1 (Fig. 1C). Next, we determined the effects of GDI-1 expression on SRE activation induced by transduction of the constitutively active RhoA mutant protein (V14RhoA). HPAE cells transducing V14RhoA had a fivefold increase in SRE reporter gene activity over control cells, whereas coexpression of FL GDI-1 prevented V14RhoA-induced SRE activation (Fig. 1D).

The GDI-1 C terminus regulates RhoA activation. GDI-1 is composed of a flexible 69-aa N terminus and a folded 135-aa C terminus (3, 6, 23). We have shown that thrombin-induced PKCα phosphorylation of GDI-1 mediates the activation of RhoA (23). Since in unstimulated cells GDI-1 is present as a GDI-RhoA complex, we determined whether GDI-1 complexed with RhoA is the preferred substrate for PKCα. COS-7
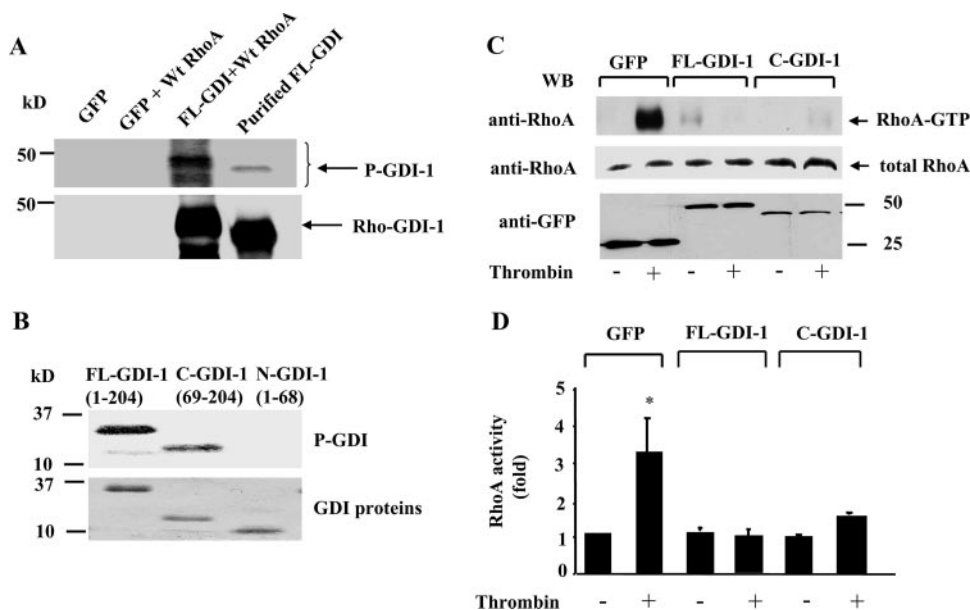
FIG. 2. Effect of FL GDI-1 or the C terminus of GDI-1 on thrombin-induced RhoA activity. (A) Autoradiogram showing PKCα-induced phosphorylation of the GDI-1–RhoA complex or the purified GDI-1 protein in vitro. COS-7 cells were cotransduced with the control vector (GFP) or GFP–GDI-1 along with WT RhoA, and after 48 h the lysates were immunoprecipitated with anti-GFP Ab, followed by the addition of protein A/G plus beads. Immunocomplexes, as well as purified GDI-1 protein, were used for in vitro phosphorylation by PKCα as described in Materials and Methods. PKCα induced a greater increase in the phosphorylation of the GDI-1–RhoA complex compared to the purified FL GDI-1 protein. The bottom part of the panel shows the protein loading determined by Western blotting with anti-GDI-1 Ab. An extra band in lane 3 represents the heavy chain of IgG. Data are representative of three independent experiments. (B, top) Autoradiogram showing PKCα phosphorylation of the C terminus but not the N terminus of GDI-1. Purified FL GDI-1 and GDI-1 lacking the C terminus (aa 69 to 204) or the N terminus (aa 1 to 68) were incubated with PKCα in vitro, and phosphorylation was determined as described in Materials and Methods. (B, bottom) Equal protein loading determined by Coomassie blue staining of GDI-1 proteins. (C and D) RhoA activity in response to thrombin in HPAE cells transduced with GFP or GFP-tagged FL GDI-1 or C-GDI-1 mutant. RhoA activity was determined after 2 min of thrombin stimulation. RhoA activation was measured by the increase in the amount of GTP-bound RhoA (C, top) compared to the total amount of RhoA in whole-cell lysates (C, middle). The bottom of panel C shows the expression of GDI-1 mutant proteins determined by Western blotting (WB) with anti-GFP Ab. (D) Plot showing mean values ± standard deviations for the thrombin-induced increase in RhoA activity from multiple experiments calculated as the n-fold increase over the basal value under different experimental conditions (n = 3). Asterisks indicate values different from those obtained with unstimulated, vector-expressing cells or cells expressing FL or C-GDI-1 with or without thrombin stimulation (P < 0.05). +, presence; −, absence.

cells were cotransduced with GFP-tagged FL GDI-1 with or without wild-type (WT) RhoA. Lysates from COS-7 cells were immunoprecipitated with anti-GFP Ab to obtain the GDI-1–RhoA immunocomplex. The immunocomplex and purified GST–GDI-1 were used for in vitro kinase assays. As shown in Fig. 2A, PKCα induced greater phosphorylation of the GDI-RhoA complex than GDI-1 alone. To address whether GDI-1 phosphorylation regulates the inhibitory activity of GDI-1 on Rho GTPases, we first identified the GDI-1 region subject to phosphorylation by PKCα. Upon the incubation of purified FL GDI-1, GDI-1 N-terminal (1 to 68), or GDI-1 C-terminal (69 to 204) protein with PKCα in vitro, we observed that PKCα only phosphorylated the C terminus of GDI-1 (Fig. 2B).

Because the C terminus of GDI-1 binds Rho GTPases (9), we addressed whether a truncated GDI-1 mutant protein containing the C terminus would alter RhoA activation following thrombin stimulation. HPAE cells were transduced with FL GDI-1 or C-GDI mutant construct, and RhoA activity was determined with rhotekin-bound fusion proteins. Thrombin failed to induce RhoA activity in endothelial cells transducing FL GDI-1 (Fig. 2C and D), as well as in cells transducing the C-GDI-1 mutant construct (Fig. 2C and D).

Since intermolecular interaction in C-GDI-1 via two antiparallel β-sheets (9, 11) may limit C-GDI-1 phosphorylation and

hence RhoA activation, we further truncated the C terminus to generate GFP-tagged C1 (aa 69 to 140) and C2 (aa 141 to 204) mutant constructs. GFP-tagged C1- or C2-GDI-1 mutant constructs were expressed in COS-7 cells, and immunocomplexes were phosphorylated with PKCα to determine whether the truncations affected PKCα phosphorylation of the C terminus. As shown in Fig. 3A, PKCα phosphorylation of C1-GDI-1 was greater than that of C2-GDI-1. Next, C-, C1-, and C2-GDI-1 mutant constructs were transduced in HPAE cells to determine their effects on thrombin-induced SRE activation. Thrombin failed to induce SRE activity in endothelial cells transducing the C terminus (Fig. 3B). However, truncations of the C terminus prevented its inhibitory activity on RhoA; that is, thrombin-induced SRE activation was not affected in HPAE cells transducing the C1- or C2-GDI-1 mutant construct (Fig. 3B). To address the possibility that the increased SRE activity in C1- and C2-GDI-1-expressing cells was due to their reduced binding to RhoA, we coexpressed WT RhoA together with either the C-, C1-, or C2-GDI-1 mutant construct in COS7 cells and carried out coimmunoprecipitation assays. GDI-1 immunoprecipitated RhoA in cells expressing either the C-GDI-1 or C1-GDI-1 mutant protein, although the association was 35% less in cells transducing C1-GDI-1 than in C CDI-1-expressing cells (Fig. 3C). Also, the association of GDI-1 with
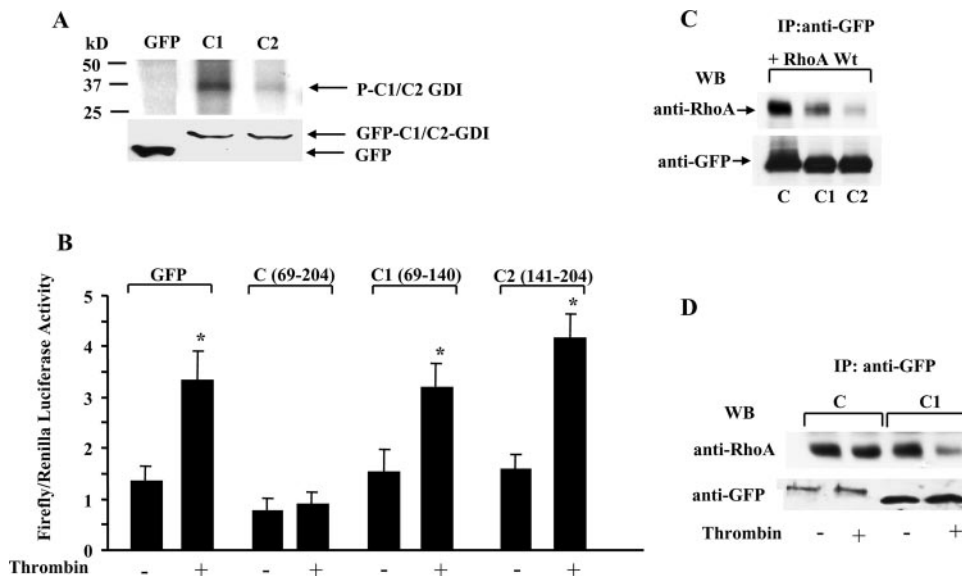
FIG. 3. PKCα-induced phosphorylation of the C terminus regulates thrombin-induced SRE generation. (A, top) Autoradiogram showing PKCα-induced phosphorylation of C1- and C2-GDI-1 mutant proteins in vitro. COS-7 cells were transduced with the indicated mutant constructs, and after 48 h the lysates were immunoprecipitated with anti-GFP Ab, followed by addition of protein A/G plus beads. The immunocomplexes were used for in vitro phosphorylation by PKCα as described in Materials and Methods. PKCα induced greater phosphorylation of the C1 domain of GDI-1 compared to the C2 domain. (A, bottom) Western blot assay with anti-GFP Ab indicating equal protein loading. Data are representative of three independent experiments. (B) SRE activity in HPAE cells transduced with the C-, C1-, or C2-GDI-1 mutant construct. HPAE cells were cotransfected with an SRE-luciferase plasmid and GFP or the indicated GFP-tagged C-, C1-, or C2-GDI-1 mutant construct. Cells were then stimulated with thrombin for 5 h prior to SRE activity measurement with the dual-reporter assay kit. SRE-luciferase activity is expressed as the ratio of firefly to *Renilla* luciferase activities in response to thrombin. Data represent the mean ± the standard deviation from four experiments performed in triplicate. Asterisks indicate values different from those obtained with unstimulated vector-expressing cells or cells expressing the indicated GDI-1 mutant proteins ($P < 0.05$). +, presence; −, absence. (C) Association of RhoA with C-, C1-, or C2-GDI-1 mutant protein. COS7 cells were cotransfected with equal concentrations of GFP-tagged C-, C1-, or C2-GDI-1 mutant construct along with HA-tagged WT RhoA (RhoA). After 48 h, cell lysates were immunoprecipitated (IP) with anti-GFP Ab, followed by Western blotting (WB) with anti-HA or anti-GFP Abs to determine the association of GDI-1 with RhoA. Data represent results from at least three experiments. The bottom of the panel shows a Western blot assay with anti-GFP Ab indicating mutant protein expression. (D) HPAE cells transduced with the C or C1-GDI-1 mutant construct were stimulated with thrombin for 2 min, and lysates were immunoprecipitated with anti-GFP Ab, followed by Western blotting with anti-RhoA or anti-GFP Abs. Data represent results from at least two experiments. +, presence; −, absence.

RhoA was markedly reduced in cells expressing C2-GDI-1 compared to that in cells expressing C1-GDI-1. Since both C-GDI-1 and C1-GDI-1 bind RhoA, we determined whether thrombin induced RhoA activity in C1-GDI-1-expressing cells by altering the association of GDI-1 with RhoA. HPAE cells transduced with the C-GDI-1 or C1-GDI-1 mutant construct were stimulated with thrombin, and lysates were immunoprecipitated with anti-GFP Ab, followed by Western blotting with anti-RhoA Ab. We observed that in unstimulated endothelial cells RhoA associated with the C-GDI-1 and C1-GDI-1 mutant proteins (Fig. 3D), recapitulating the findings obtained with COS7 cells (Fig. 3C). However, thrombin decreased the association of RhoA in cells expressing the C1-GDI-1 mutant protein, whereas this effect was not seen in endothelial cells expressing the C-GDI-1 mutant protein (Fig. 3D).

To determine whether phosphorylation of the C1 domain was responsible for RhoA activation, we used the NetPhos program, which predicts phosphobases in GDI-1. C1-GDI-1 was found to contain a consensus PKCα phosphorylation site at residue Ser96. Residue serine 96 was replaced with alanine to generate the nonphosphorylatable S96A C1-GDI-1 mutant construct. We also mutated S176 and T197 in C2-GDI-1 to alanine to address whether the phosphorylation at these sites additionally contributed to RhoA signaling. Figure 4A shows

that PKCα failed to phosphorylate the S96A-GDI-1 mutant protein, whereas phosphorylation of C2 fragments containing the S176A or S197A mutation persisted, although at reduced levels. We observed that only S96A-GDI-1 mutant protein expression prevented SRE activation in HPAE cells in response to thrombin (Fig. 4B). Further, thrombin-induced RhoA activation was markedly suppressed in HPAE cells expressing the S96A-GDI-1 mutant protein (Fig. 4C and D). Thrombin also failed to decrease the association of RhoA in cells expressing the S96A C1 mutant protein (Fig. 4E).

To corroborate these findings, thrombin-induced RhoA activation was also determined in endothelial cells expressing FL GDI-1 mutant proteins in which S96, S176, or T197 was replaced with alanine. As shown in Fig. 5A, mutating S96, S176, or T197 to alanine reduced GDI-1 phosphorylation to almost the same extent. However, GDI-1 phosphorylation at residue S96 was required for RhoA activation since thrombin failed to induce SRE activity in cells transduced with FL GDI-1-S96A but not in cells transduced with the FL S176A-GDI-1 or FL T197A-GDI-1 mutant construct (Fig. 5B and D). Moreover, a GDI-1 phospho-mimicking mutant protein in which Ser96 was replaced with Asp (S96D) significantly increased SRE activity without thrombin stimulation (Fig. 5C). Expression of the S96D-GDI-1 mutant protein also significantly increased basal
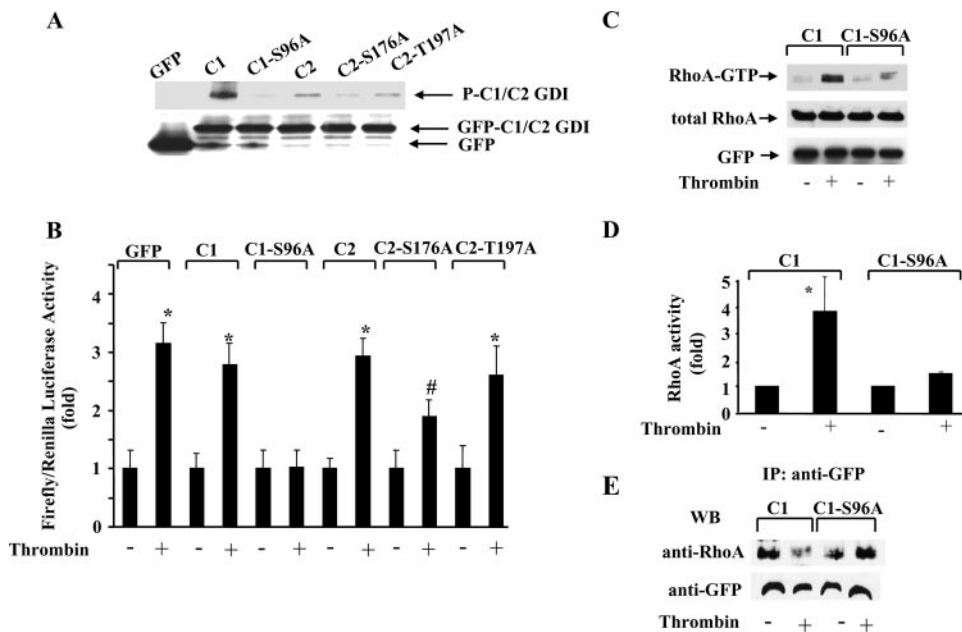
FIG. 4. Effects of nonphosphorylatable truncated GDI-1 mutant proteins on SRE and RhoA activities in response to thrombin. (A) Mutation of Ser96, Ser176, and Thr197 to alanine reduced the phosphorylation of the C1 and C2 domains by PKCα in vitro. COS-7 cells transduced with the indicated mutant constructs were immunoprecipitated with anti-GFP Ab and complexed with protein A/G plus beads. Immunocomplexes were used for in vitro phosphorylation by PKCα as described in Materials and Methods. The top of the panel shows an autoradiograph of a gel, whereas the bottom of the panel shows GFP-tagged protein expression determined by Western blotting with anti-GFP Ab. Data are representative of three independent experiments. (B) HPAE cells cotransfected with the indicated GFP-tagged mutant constructs were stimulated with thrombin for 5 h prior to SRE activity measurement with a dual-reporter assay kit. SRE-luciferase activity is expressed as the ratio of firefly to *Renilla* luciferase activities quantified as the percent increase in SRE activity over that in unstimulated cells. Data represent the mean ± the standard deviation from three experiments performed in triplicate. The symbols ∗ and # indicate increased SRE activity compared to that obtained with unstimulated cells (∗, $P < 0.01$; #, $P < 0.05$). (C) HPAE cells transduced with the C1- or S96A-C1-GDI-1 mutant construct were stimulated with 50 nM thrombin for 2 min to determine RhoA activity with GST-bound rhotekin fusion proteins. RhoA activation was measured by the increased amount of GTP-bound RhoA (top) compared to that of RhoA in whole-cell lysates (middle). A Western blot assay with anti-GFP Ab shows mutant protein expression (bottom). (D) Plot showing the mean ± the standard deviation of the thrombin-induced increase in RhoA activity from multiple experiments calculated as the *n*-fold increase over the basal value under various experimental conditions ($n = 3$). An asterisk indicates an increase in RhoA activity compared to that of a vector-transfected unstimulated monolayer and cells expressing the S96A-C1 mutant protein ($P < 0.05$). (E) HPAE cells transduced with the C1 or S96A-C1 mutant construct were stimulated with thrombin for 2 min, and lysates were immunoprecipitated (IP) with anti-GFP Ab, followed by Western blotting (WB) with anti-RhoA or anti-GFP Abs. Data represent results from at least two experiments. Symbols in panels B to E: +, presence; −, absence.

RhoA activity, which slightly increased further following thrombin stimulation (Fig. 5D).

To address whether GDI-1 phosphorylation altered the binding affinity of GDI-1 for RhoA and increased the release of RhoA from the GDI-RhoA complex, thereby inducing RhoA signaling, we transduced the FL, FL S96A-, FL S176A-, FL T197-, or FL S96D-GDI-1 mutant construct into HPAE cells and determined by coimmunoprecipitation assay the association of RhoA with GDI-1 following thrombin stimulation. Increased association of GDI-1 with RhoA was seen in cells expressing FL GDI-1 or FL S96A-GDI-1 (Fig. 5E). However, GDI-1 association with RhoA was decreased in cells transduced with S176A-GDI-1 and barely detectable in cells transduced with the T197A-GDI-1 mutant (Fig. 5E). Moreover, thrombin decreased the association of RhoA with GDI-1 in cells expressing the FL S176A-GDI-1 mutant protein but not in cells transducing the S96A-GDI-1 or FL GDI-1 mutant protein (Fig. 5E). In contrast, RhoA interaction with GDI-1 was not evident in cells expressing the S96D mutant protein. Since it is possible that increased ectopic expression in HPAE cells may have forced the interaction between GDI-1 and

RhoA, we used COS7 cells to coexpress equal amounts of WT RhoA along with the empty vector or the GFP-tagged S96A- or S96D-GDI-1 mutant construct and repeated the above-described studies. We observed that the association of GDI-1 with RhoA was markedly reduced in cells expressing the S96D-GDI-1 mutant protein in comparison to cells expressing the S96A-GDI-1 mutant protein (Fig. 5F). These findings support the model in which phosphorylation of the C terminus of GDI-1 at S96 is crucial in decreasing its binding affinity for RhoA and thereby inducing RhoA activation and RhoA-dependent SRE activation.

Phosphodefective truncated and FL S96A-GDI-1 mutant proteins fail to prevent Rac1 or Cdc42 activation. Thrombin activation of endothelial cells induces transient activation of RhoA (12, 19). Rac1 was shown to be inactivated (15, 35), whereas thrombin induced delayed activation of Cdc42 (15). We determined Rac1 and Cdc42 activities in HPAE cells transduced with either the truncated C1-S96A-GDI-1 mutant construct or the FL S96A-GDI-1 mutant construct to assess whether mutation of Ser96 also altered the activation of these GTPases in response to thrombin. As shown in Fig. 6A to D,
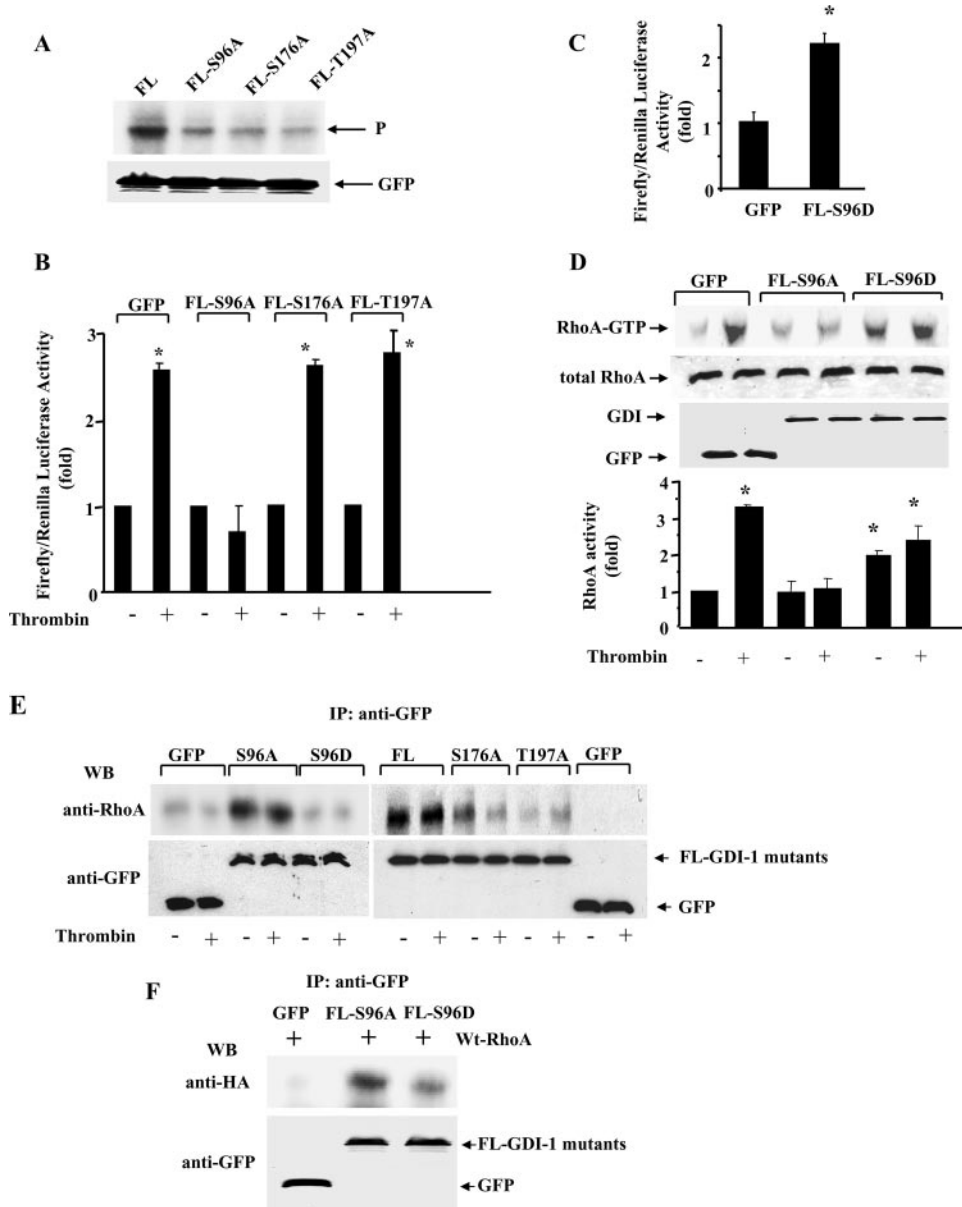
FIG. 5. Phosphorylation of Ser96 is required for SRE and RhoA activation. (A) Mutation of Ser96, Ser176, and Thr197 to alanine markedly reduced the phosphorylation of FL GDI-1 by PKCα in vitro. COS-7 cells transduced with the indicated mutant constructs were immunoprecipitated with anti-GFP Ab and complexed with protein A/G plus beads. Immunocomplexes were used for in vitro phosphorylation by PKCα as described in Materials and Methods. The top of the panel shows the autoradiograph of the gel, whereas the bottom of the panel shows protein expression determined by Western blotting with anti-GFP Ab. Data are representative of three independent experiments. (B) HPAE cells cotransfected with the indicated GFP-tagged mutant proteins were stimulated with thrombin for 5 h prior to SRE activity measurement with a dual-reporter assay kit. SRE-luciferase activity is expressed as the increase in the ratio of firefly to *Renilla* luciferase activities quantified as an *n*-fold increase in SRE activity over that in unstimulated cells. Data represent the mean ± the standard deviation from three experiments performed in triplicate. An asterisk indicates increased SRE activity compared to that in unstimulated vector-expressing cells or cells expressing the S96A-GDI-1 mutant protein with or without thrombin ($P < 0.05$). +, presence; −, absence. (C) HPAE cells were cotransfected with the GFP or S96D-GDI-1 mutant construct, and after 24 h, SRE activity was determined with a dual-reporter assay kit. SRE-luciferase activity is expressed as the ratio of firefly to *Renilla* luciferase activities quantified as the *n*-fold increase in SRE activity over that in GFP-transfected cells. Data represent the mean ± the standard deviation from three experiments performed in triplicate. An asterisk indicates increased SRE activity compared to that in a GFP-transfected monolayer ($P < 0.05$). (D) HPAE cells transduced with GFP or the S96A- or S96D-GDI-1 mutant construct were stimulated with 50 nM thrombin for 2 min to determine RhoA activity with GST-bound rhotekin fusion proteins. The Western blot assay at the top shows RhoA activity measured by the increased amount of GTP-bound RhoA compared to GFP expression. At the bottom is a plot of the mean ± the standard deviation of the thrombin-induced increase in RhoA activity from multiple experiments calculated as the *n*-fold increase over the basal value under various experimental conditions ($n = 3$). An asterisk indicates an increase in RhoA activity compared to that in an unstimulated monolayer ($P < 0.05$). (E and F) Phosphorylation of GDI-1 increased the affinity of GDI-1 for RhoA. (E) HPAE cells transduced with GFP, GFP-tagged FL GDI-1, or the GFP-tagged S96A-, S176A-, T197A-, or S96D-GDI-1 mutant construct were stimulated with thrombin for 2 min, and lysates were immunoprecipitated (IP) with anti-GFP Ab, followed by Western blotting (WB) with anti-RhoA or anti-GFP Ab. Data represent results from at least two experiments. (F) COS7 cells were cotransduced with a GFP or a GFP-tagged S96A- or S96D-GDI-1 mutant construct together with HA-tagged WT RhoA. After 42 h, the lysates were immunoprecipitated with anti-GFP Ab, followed by Western blotting with anti-HA or anti-GFP Ab. Data represent results from at least three experiments. +, presence; −, absence.
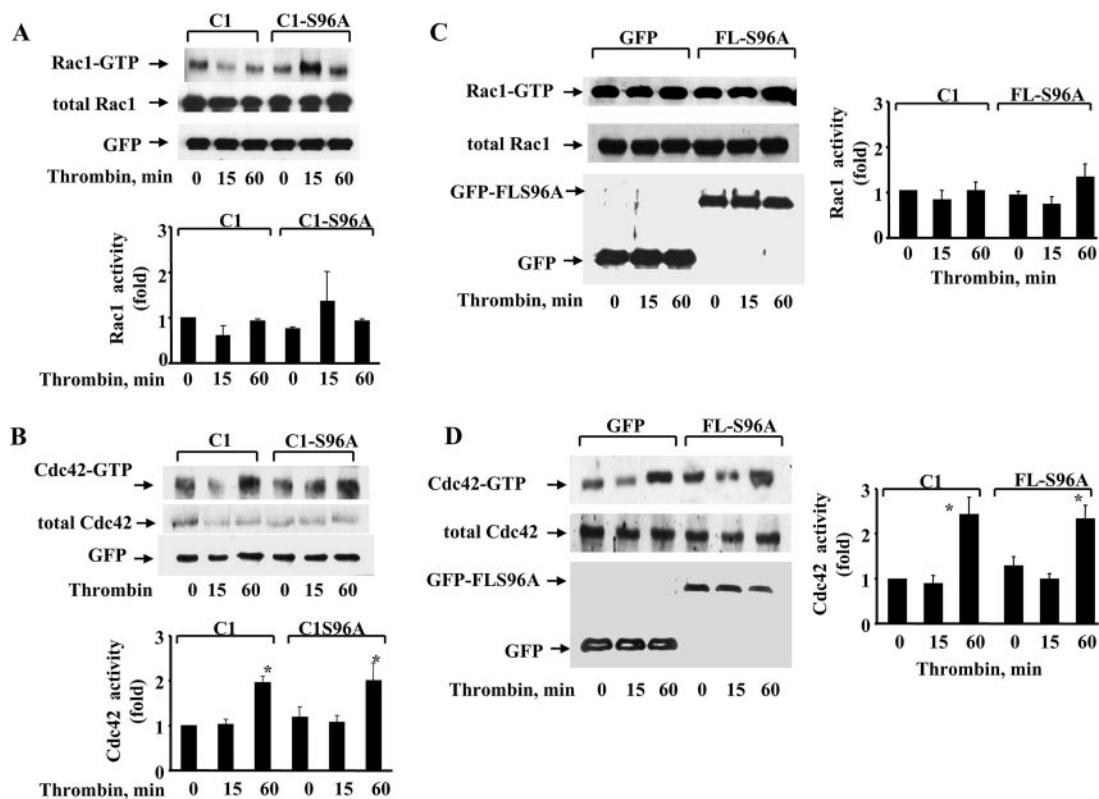
FIG. 6. S96A-GDI-1 mutant protein fails to inhibit Rac1 or Cdc42 activity. (A to D) HPAE cells transduced with the C1-GDI-1 or S96A-C1-GDI-1 mutant construct (A and B) or GFP or the FL S96A-GDI-1 mutant construct (C and D) were stimulated with 50 nM thrombin for the indicated times to determine Rac1 (A and C) or Cdc42 activity (B and D) with GST-bound PAK-binding domain fusion proteins. Rac1 and Cdc42 activation was measured by the increased amount of GTP-bound Rac1 (A and C, top) or GTP-bound Cdc42 (B and D) compared to that of Rac1 or Cdc42 in whole-cell lysates (A to D). A Western blot assay with anti-GFP Ab shows mutant protein expression (A to D, bottom). Data represent results from at least three experiments. The plots in panels A to D show the mean ± standard deviation of thrombin-induced changes in Rac1 or Cdc42 activity from multiple experiments calculated as the n-fold increase over the basal value under the indicated experimental conditions (n = 3). An asterisk indicates increased Cdc42 activity in cells expressing the indicated mutant proteins following thrombin stimulation ($P < 0.05$).

expression of either the truncated C1-S96A-GDI-1 (Fig. 6 A and B) or the FL S96A-GDI-1 (Fig. 6C and D) mutant protein in HPAE cells had no effect on thrombin-induced alterations of Rac1 and Cdc42 activities; thus, the S96A-GDI-1 mutation selectively prevents RhoA activation.

Phosphodefective truncated and FL S96A-GDI-1 mutant proteins inhibit actin stress fiber formation and increased endothelial permeability induced by thrombin. Because RhoA activation increased endothelial permeability by inducing myosin light chain (MLC) phosphorylation and actin stress fiber formation (19), we determined the requirement for GDI-1 phosphorylation at Ser96 in mediating thrombin-induced actin stress fiber formation and MLC phosphorylation. We also determined changes in TER to address the role of S96 phosphorylation in regulating endothelial barrier function. As shown in Fig. 7A to D, thrombin induced MLC phosphorylation and increased stress fiber formation, as well as TER, in cells transduced with the GFP- or C1-GDI-1 mutant construct; however, these responses were markedly decreased in cells expressing the C1-S96A- or FL S96A-GDI-1 mutant protein (Fig. 7A to D). Inhibition of PKCα with Gö6976 (13) significantly reduced the thrombin-induced decrease in TER in HPAE cells expressing the C1-GDI-1 mutant protein (normalized resistance; 0.51 ± 0.003 to 0.33 ± 0.017 Ω; $P < 0.05$), whereas this

response was abrogated in cells expressing the S91A-GDI-1 mutant protein (0.28 ± 0.002 to 0.27 ± 0.017 Ω; $P > 0.05$). Further, expression of the phospho-mimicking GDI-1 (S96D-GDI-1) mutant protein independently increased endothelial permeability (Fig. 7E). Thus, PKCα phosphorylation of GDI-1 at residue serine 96 is a critical requirement for thrombin-induced RhoA activation and in signaling the increase in endothelial permeability.

DISCUSSION

GDI-1, by binding to Rho GTPases, inhibits their activation and thereby regulates downstream Rho GTPase-mediated signaling (3, 5, 6, 23). GDI-1 consists of structurally different N and C termini. In vitro studies showed that a GDI-1 mutant protein containing only the C terminus binds Rho GTPases (9) and that posttranslational modification within the C-terminal domain of GDI-1 altered its Rac1 inhibitory activity (4). We have previously shown that PKCα phosphorylates GDI-1 (20). In the present study, we addressed the GDI-1-dependent mechanism of RhoA activation and the role of GDI-1 in mediating increased endothelial permeability. Studies were done with FL GDI-1 and GDI-1 C-terminal mutant constructs (C-GDI). Our findings have identified the critical role of the C
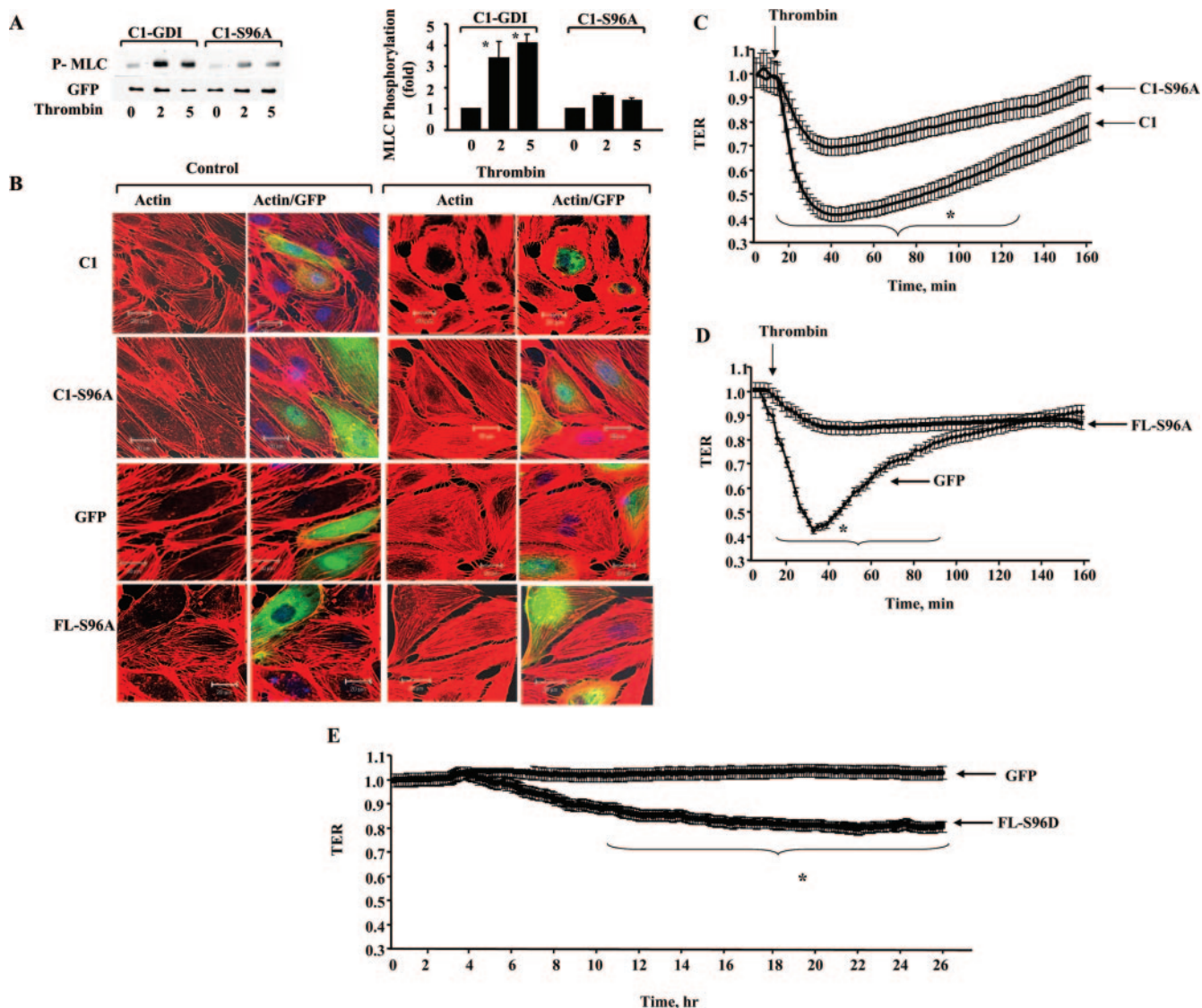
FIG. 7. Effects of GDI-1 phosphorylation on MLC phosphorylation, actin stress fiber formation, and increased endothelial permeability in response to thrombin. (A) MLC phosphorylation in response to thrombin in cells transduced with a C1- or C1-S96A-GDI-1 mutant construct. Cells were stimulated with thrombin for the indicated times (indicated in minutes below the lanes), and lysates were Western blotted with anti-phospho-MLC (top) or anti-GFP Abs to determine MLC phosphorylation. The plot shows the mean ± the standard deviation of the thrombin-induced increase in MLC phosphorylation from multiple experiments calculated as the *n*-fold increase over the basal value under the indicated experimental conditions ($n = 3$). An asterisk indicates increased MLC phosphorylation in cells expressing the indicated mutant proteins following thrombin stimulation ($P < 0.05$). (B) Actin stress fiber formation in response to thrombin in cells transduced with a GFP-tagged C1-GDI-1, C1-S96A-GDI-1, or FL S96A-GDI-1 mutant construct. Cells were stimulated with thrombin for 5 min, fixed, and then stained with Alexa-labeled phalloidin to determine actin stress fiber formation by confocal imaging. Results are representative of at least four experiments. (C) Cells plated on gold electrodes were transduced with a C1- or C1-S96A-GDI-1 mutant construct to measure the time course of changes in TER after the addition of 50 nM thrombin. Data represent the means ± the standard deviations of changes in TER from multiple experiments. An asterisk indicates a significant decrease in TER in cells expressing C1-S96A-GDI-1 compared to that of cells transducing the C1-GDI-1 mutant protein ($P < 0.05$). (D) Means ± standard deviations of changes in TER in HPAE cells expressing GFP or the FL S96A-GDI-1 mutant protein. After 30 h posttransfection, cells were stimulated with 50 nM thrombin and changes in TER were monitored. An asterisk indicates a significant decrease in TER in cells expressing the FL S96A-GDI-1 mutant protein compared to that of cells transducing the empty vector ($P < 0.05$). (E) Cells plated on gold electrodes were transduced with GFP or the FL S96D-GDI-1 mutant construct and after 2 h posttransfection, the time course of changes in TER was determined. Data represent the means ± the standard deviations of changes in TER from multiple experiments. An asterisk indicates a significant increase in TER in cells transduced with the FL S96D-GDI-1 mutant protein compared to that of cells transduced with the empty vector ($P < 0.05$).

terminus of GDI-1 in regulating RhoA signaling and the RhoA-dependent increase in endothelial permeability.

Thrombin binds and cleaves PAR-1 in endothelial cells, leading to the activation of heterotrimeric G proteins $G\alpha_{12}$, $G\alpha_{13}$, and $G\alpha_q$ (2). The released α subunits of $G\alpha_q$ and $G\alpha_{12}$/$G\alpha_{13}$ were shown to induce RhoA activation (1, 13, 16, 25, 34). We observed that GDI-1 prevented RhoA activation and actin stress fiber formation in response to thrombin stimulation of

endothelial cells, consistent with the role of GDI-1 in the binding and inactivation of RhoA (3, 6, 23). We further showed that GDI-1 inhibited RhoA activation induced by the constitutively active Gα$_{12}$, Gα$_{13}$, and Gα$_q$ mutant proteins, indicating the central role of GDI-1 in regulating RhoA activity downstream of G-protein-coupled receptors. Other studies have shown that microinjection of GDI-1 in fibroblasts and MDCK cells inhibited RhoA-induced cell motility, formation of stress fibers, and development of focal adhesions (14, 29–32). To address whether GDI-1 is capable of inhibiting active RhoA, we used the constitutively active V14RhoA mutant protein, which retains all of the features of WT RhoA except that mutation of Gly14 to Val eliminates its GTPase activity (7, 22, 24). V14RhoA also binds its effectors and activates downstream signaling (7, 22, 24). We observed that GDI-1 expression prevented the signaling induced by expression of the constitutively active V14RhoA mutant protein, indicating that GDI-1 can bind the active RhoA protein and holds it in abeyance.

To identify the domain(s) of GDI-1 responsible for regulating RhoA activity, we focused on the C terminus. We observed that expression of the C-GDI-1 mutant protein (aa 69 to 204) in endothelial cells prevented RhoA activation in response to thrombin. C-GDI-1 was shown to associate with RhoA in endothelial cells, as well as in COS7 cells expressing C-GDI-1. On the basis of structural findings that two antiparallel β-sheets of the C terminus fold to form a Rho GTPase binding pocket (9, 11), our findings are consistent with the model in which C-GDI-1 sequestration of RhoA in the GTPase binding pocket region restricts its activation.

Studies have shown that phosphorylation of GDI-1 prevented its inhibitory activity against Rac1 (4). We observed that GDI-1 complexed with RhoA was a preferred substrate for PKCα over GDI-1 alone. Also, PKCα was directly capable of phosphorylating the C terminus of GDI-1. We had expected that C-GDI-1 phosphorylation would enable RhoA activation; however, in cells expressing C-GDI-1, thrombin failed to induce the dissociation of RhoA from C-GDI-1 and thereby did not induce RhoA activation. The basis of this finding is not clear. Since the C terminus of GDI-1 can acquire a folded conformation via the interaction of two antiparallel β-sheets (9, 11), the phosphorylation sites may be masked in the GDI-1 mutant protein, thus limiting RhoA activation. Supporting this view, our data showed that truncation of C-GDI-1 into C1 (aa 69 to 140) and C2 (aa 141 to 204) fragments enabled RhoA activation following marked phosphorylation of the C1 domain. RhoA was also shown to associate with C1-GDI-1 in the cells expressing this mutant protein, although with an affinity less than that for C-GDI-1. Moreover, thrombin decreased the association of RhoA with C1-GDI-1, thus enabling RhoA activation, in contrast to the C-GDI-1-expressing cells. The affinity for RhoA was the least in the C2-GDI-1 mutant protein-expressing cells. The latter finding may be the result of impaired binding via the isoprenyl group of Rho GTPases in the absence of Gln130 in the C2 mutant protein. Replacement of S96 with Ala in C1-GDI-1, as well as in FL GDI-1 mutant proteins, which inhibited phosphorylation, prevented RhoA activation. However, mutating the S176 or T917 residue in FL GDI-1 to Ala failed to alter thrombin-induced SRE activity because of a decreased interaction of GDI-1 with RhoA. It is

possible that mutation of the S176 or T197 residue in FL GDI-1 may have altered the topology of the expressed protein such that its affinity for RhoA was decreased, enabling thrombin to induce SRE activity. These findings demonstrate that S96 at the C terminus of GDI-1 plays a critical role in regulating RhoA activity; thus, induction of phosphorylation at Ser96 by thrombin results in RhoA activation.

The mechanism of RhoA activation induced by GDI-1 phosphorylation at S96 is not clear. Structural data showed that conserved hydrophobic residues located inside the Rho GTPase binding pocket form van der Waals interactive forces between GDI-1 and the geranylgeranyl group of RhoA (11). Phe102 is predicted to form contacts with both Trp194 and Leu77 in the two opposing β-sheets of GDI-1 (11). Thus, phosphorylation of the S96 residue, which is near Phe102, may induce conformational changes within the Rho GTPase binding pocket that reduce the affinity of RhoA and dissociate it from GDI-1 (11).

We also show that although the phospho-mimicking S96D-GDI-1 mutant protein did not bind RhoA, it increased SRE and RhoA activities in the absence of thrombin stimulation. GDI-1 has been shown to interact with ERM proteins such as radixin (27), Grail, a ubiquitin ligase (26), and the β8 subunit of integrin (17). Whereas ERM binding with GDI-1 induces RhoA activation (27), Grail interaction with GDI-1 leads to inhibition of RhoA, but not Rac or Cdc42, activity (26). GDI-1 interaction with β8 has been shown to induce Rac activity (17). Thus, we can speculate that phospho-mimicking GDI-1 (FL S96D-GDI-1), by competing with Grail, may have altered the stability of the endogenous GDI-1–RhoA complex, facilitating RhoA activation. Alternatively, the S96D-GDI-1 mutant protein may have triggered an interaction between GDI-1 and ERM proteins and/or induced integrin clustering, which in turn, by displacing RhoA from the endogenous GDI-1–RhoA complex, promoted RhoA activation.

Because in vitro studies have shown that GDI-1 binds to RhoA, Rac1, and Cdc42 and inhibits their GTPase activities, GDI-1 may be a nonspecific inhibitor of activation of all Rho GTPases (3, 5, 6). However, our evidence indicates otherwise. We observed that C-terminal phosphorylation of GDI-1 selectively altered GDI-1 inhibition of RhoA activity. Phosphorylation of Ser96 induced the activation of RhoA but not Rac or Cdc42. The mechanism by which phosphorylation of GDI-1 at Ser96 specifically modifies the ability of GDI-1 to regulate RhoA activity is unclear. It is possible that charge differences attributed to Ser96 determine the binding affinity of GDI-1 for RhoA (3, 6, 23).

As RhoA activation is known to increase endothelial permeability, a hallmark of inflammatory diseases such as acute lung injury (19), we addressed the possibility that Ser96 phosphorylation of GDI-1 has a functional role in regulating the increased endothelial permeability response to a thrombin challenge. We observed that expression of the nonphosphorylatable S96A-GDI-1 mutant protein significantly inhibited MLC phosphorylation, actin stress fiber formation, and the increase in endothelial permeability induced by thrombin. The reduction in the endothelial permeability response observed in S96A-GDI-1 mutant protein-expressing endothelial cells was recapitulated by inhibiting PKCα activation in endothelial cells transduced with the C1-GDI-1 mutant construct. Thus, PKCα-induced GDI-1 phosphorylation at Ser96 is a requirement for

RhoA-induced disruption of the endothelial barrier. Drugs targeting S96 of GDI-1 may represent a novel class of antiinflammatory therapeutics to prevent increased endothelial permeability in inflammatory diseases.

In conclusion, we have identified the critical role of Ser96 in the C terminus of GDI-1 in regulating RhoA activity. Phosphorylation at Ser96 reduced the affinity of GDI-1 for RhoA and thereby selectively activated RhoA. Phosphorylation of Ser96 in the C terminus of GDI-1 represents a novel target for regulating RhoA activity and the RhoA-dependent increase in endothelial permeability.

REFERENCES

1. **Chikumi, H., J. Vázquez-Prado, J.-M. Servitja, H. Miyazaki, and J. S. Gutkind.** 2002. Potent activation of RhoA by $G\alpha_q$ and G_q-coupled receptors. J. Biol. Chem. **277:**27130–27134.
2. **Coughlin, S. R.** 2000. Thrombin signalling and protease-activated receptors. Nature **407:**258–264.
3. **DerMardirossian, C., and G. M. Bokoch.** 2005. GDIs: central regulatory molecules in Rho GTPase activation. Trends Cell Biol. **15:**356–363.
4. **DerMardirossian, C., A. Schnelzer, and G. M. Bokoch.** 2004. Phosphorylation of RhoGDI by Pak1 mediates dissociation of Rac GTPase. Mol. Cell **15:**117–127.
5. **Dovas, A., and J. R. Couchman.** 2005. RhoGDI: multiple functions in the regulation of Rho family GTPase activities. Biochem. J. **390:**1–9.
6. **Dransart, E., B. Olofsson, and J. Cherfils.** 2005. RhoGDIs revisited: novel roles in Rho regulation. Traffic **6:**957–966.
7. **Etienne-Manneville, S., and A. Hall.** 2002. Rho GTPases in cell biology. Nature **420:**629–635.
8. **Fauré, J., and M. C. Dagher.** 2001. Interactions between Rho GTPases and Rho GDP dissociation inhibitor (Rho-GDI). Biochimie **83:**409–414.
9. **Gosser, Y. Q., T. K. Nomanbhoy, B. Aghazadeh, D. Manor, C. Combs, R. A. Cerione, and M. K. Rosen.** 1997. C-terminal binding domain of Rho GDP-dissociation inhibitor directs N-terminal inhibitory peptide to GTPases. Nature **387:**814–819.
10. **Hirao, M., N. Sato, T. Kondo, S. Yonemura, M. Monden, T. Sasaki, Y. Takai, S. Tsukita, and S. Tsukita.** 1996. Regulation mechanism of ERM (ezrin/radixin/moesin) protein/plasma membrane association: possible involvement of phosphatidylinositol turnover and Rho-dependent signaling pathway. J. Cell Biol. **135:**37–51.
11. **Hoffman, G. R., N. Nassar, and R. A. Cerione.** 2000. Structure of the Rho family GTP-binding protein Cdc42 in complex with the multifunctional regulator RhoGDI. Cell **100:**345–356.
12. **Holinstat, M., N. Knezevic, M. Broman, A. M. Samarel, A. B. Malik, and D. Mehta.** 2006. Suppression of RhoA activity by focal adhesion kinase-induced activation of p190RhoGAP: role in regulation of endothelial permeability. J. Biol. Chem. **281:**2296–2305.
13. **Holinstat, M., D. Mehta, T. Kozasa, R. D. Minshall, and A. B. Malik.** 2003. Protein kinase Cα-induced p115RhoGEF phosphorylation signals endothelial cytoskeletal rearrangement. J. Biol. Chem. **278:**28793–28798.
14. **Kotani, H., K. Takaishi, T. Sasaki, and Y. Takai.** 1997. Rho regulates association of both the ERM family and vinculin with the plasma membrane in MDCK cells. Oncogene **14:**1705–1713.
15. **Kouklis, P., M. Konstantoulaki, S. Vogel, M. Broman, and A. B. Malik.** 2004.
16. **Kozasa, T., X. Jiang, M. J. Hart, P. M. Sternweis, W. D. Singer, A. G. Gilman, G. Bollag, and P. C. Sternweis.** 1998. p115 RhoGEF, a GTPase activating protein for $G\alpha_{12}$ and $G\alpha_{13}$. Science **280:**2109–2111.
17. **Lakhe-Reddy, S., S. Khan, M. Konieczkowski, G. Jarad, K. L. Wu, L. F. Reichardt, Y. Takai, L. A. Bruggeman, B. Wang, J. R. Sedor, and J. R. Schelling.** 2006. β8 integrin binds Rho GDP dissociation inhibitor-1 and activates Rac1 to inhibit mesangial cell myofibroblast differentiation. J. Biol. Chem. **281:**19688–19699.
18. **Lian, L. Y., I. Barsukov, A. P. Golovanov, D. I. Hawkins, R. Badii, K. H. Sze, N. H. Keep, G. M. Bokoch, and G. C. Roberts.** 2000. Mapping the binding site for the GTP-binding protein Rac-1 on its inhibitor RhoGDI-1. Structure **8:**47–55.
19. **Mehta, D., and A. B. Malik.** 2006. Signaling mechanisms regulating endothelial permeability. Physiol. Rev. **86:**279–367.
20. **Mehta, D., A. Rahman, and A. B. Malik.** 2001. Protein kinase C-α signals rho-guanine nucleotide dissociation inhibitor phosphorylation and rho activation and regulates the endothelial cell barrier function. J. Biol. Chem. **276:**22614–22620.
21. **Moers, A., N. Wettschureck, S. Gruner, B. Nieswandt, and S. Offermanns.** 2004. Unresponsiveness of platelets lacking both $G\alpha_q$ and $G\alpha_{13}$. Implications for collagen-induced platelet activation. J. Biol. Chem. **279:**45354–45359.
22. **Nobes, C. D., and A. Hall.** 1999. Rho GTPases control polarity, protrusion, and adhesion during cell movement. J. Cell Biol. **144:**1235–1244.
23. **Olofsson, B.** 1999. Rho guanine dissociation inhibitors: pivotal molecules in cellular signalling. Cell Signal. **11:**545–554.
24. **Ridley, A. J.** 1999. Rho family proteins and regulation of the actin cytoskeleton. Prog. Mol. Subcell. Biol. **22:**1–22.
25. **Singh, I., N. Knezevic, G. U. Ahmmed, V. Kini, A. B. Malik, and D. Mehta.** 2007. $G\alpha_q$-TRPC6-mediated Ca^{2+} entry induces RhoA activation and resultant endothelial cell shape change in response to thrombin. J. Biol. Chem. **282:**7833–7843.
26. **Su, L., N. Lineberry, Y. Huh, L. Soares, and C. G. Fathman.** 2006. A novel E3 ubiquitin ligase substrate screen identifies Rho guanine dissociation inhibitor as a substrate of gene related to anergy in lymphocytes. J. Immunol. **177:**7559–7566.
27. **Takahashi, K., T. Sasaki, A. Mammoto, K. Takaishi, T. Kameyama, S. Tsukita, and Y. Takai.** 1997. Direct interaction of the Rho GDP dissociation inhibitor with ezrin/radixin/moesin initiates the activation of the Rho small G protein. J. Biol. Chem. **272:**23371–23375.
28. **Takai, Y., T. Sasaki, and T. Matozaki.** 2001. Small GTP-binding proteins. Physiol. Rev. **81:**153–208.
29. **Takaishi, K., A. Kikuchi, S. Kuroda, K. Kotani, T. Sasaki, and Y. Takai.** 1993. Involvement of rho p21 and its inhibitory GDP/GTP exchange protein (rho GDI) in cell motility. Mol. Cell. Biol. **13:**72–79.
30. **Takaishi, K., T. Sasaki, T. Kameyama, S. Tsukita, S. Tsukita, and Y. Takai.** 1995. Translocation of activated Rho from the cytoplasm to membrane ruffling area, cell-cell adhesion sites and cleavage furrows. Oncogene **11:**39–48.
31. **Takaishi, K., T. Sasaki, M. Kato, W. Yamochi, S. Kuroda, T. Nakamura, M. Takeichi, and Y. Takai.** 1994. Involvement of Rho p21 small GTP-binding protein and its regulator in the HGF-induced cell motility. Oncogene **9:**273–279.
32. **Takaishi, K., T. Sasaki, H. Kotani, H. Nishioka, and Y. Takai.** 1997. Regulation of cell-cell adhesion by rac and rho small G proteins in MDCK cells. J. Cell Biol. **139:**1047–1059.
33. **Togawa, A., J. Miyoshi, H. Ishizaki, M. Tanaka, A. Takakura, H. Nishioka, H. Yoshida, T. Doi, A. Mizoguchi, N. Matsuura, Y. Niho, Y. Nishimune, S. Nishikawa, and Y. Takai.** 1999. Progressive impairment of kidneys and reproductive organs in mice lacking Rho GDIα. Oncogene **18:**5373–5380.
34. **Vogt, S., R. Grosse, G. Schultz, and S. Offermanns.** 2003. Receptor-dependent RhoA activation in G12/G13-deficient cells: genetic evidence for an involvement of $G_q/G11$. J. Biol. Chem. **278:**28743–28749.
35. **Vouret-Craviari, V., C. Bourcier, E. Boulter, and E. van Obberghen-Schilling.** 2002. Distinct signals via Rho GTPases and Src drive shape changes by thrombin and sphingosine-1-phosphate in endothelial cells. J. Cell Sci. **115:**2475–2484.
36. **Wojciak-Stothard, B., and A. J. Ridley.** 2002. Rho GTPases and the regulation of endothelial permeability. Vasc. Pharmacol. **39:**187–199.

Cdc42 regulates the restoration of endothelial barrier function. Circ. Res. **94:**159–166.